Journal of the Arkansas Academy of Science

Volume 43 Article 29

1989

Image Processing Instrumentation for Giardia lamblia Detection

Cy R. Tamanaha
University of Arkansas at Little Rock

Mark A. Gross
University of Arkansas at Little Rock

IMAGE PROCESSING INSTRUMENTATION FOR *GIARDIA LAMBLIA* DETECTION

CY R. TAMANAHA and MARK A. GROSS
University of Arkansas at Little Rock
Department of Electronics & Instrumentation
2801 South University
Little Rock, AR 72204

ABSTRACT

Currently, the identification and enumeration of *Giardia lamblia* cysts are based upon microscopic methods requiring individuals proficient in this area. It is a tedious process which consumes time that could be constructively used elsewhere. This project attempts to alleviate that burden by employing a computer to automatically process Indirect Fluorescent Antibody (IFA) prepared slides using digital image processing techniques. A computer controlled frame grabber, in conjunction with a CCD TV camera mounted on the epi-fluorescence microscope phototube, captures the light intensities of the objects in view under the microscope objective. The captured image is stored as pixels, with each pixel having a numerical value that can be altered using linear contrast enhancement and bit-slicing to emphasize the cysts and eliminate the majority of unwanted objects from the image. The altered image is then analyzed by a vector trace routine for typical area and perimeters characteristic to *Giardia lamblia* cysts. Objects in the image matching these characteristics are most likely cysts and are added to a running tally of the number of cysts present on the slide.

INTRODUCTION

Discovered by Leeuwenhoek in his own stools over 300 years ago and regarded as nonpathogenic, the organism *Giardia lamblia* has only within the last three decades been identified for its detrimental effects on public health. Giardiasis has been coined "traveler's disease", affecting travelers, campers, hunters, fishermen — anyone drinking from untreated or inadequately treated water supplies (Lin, 1985). Affliction can also occur through the fecal-oral route due to poor hygiene practices (Polis *et al.*, 1986). Individuals react to giardiasis differently. Some may be asymptomatic, others may have acute or chronic symptoms (AWWA, 1985). It remains as a leading waterborne intestinal disease in the United States (Lin, 1985).

Giardia lamblia is a single-cell flagellated protozoan having a two-stage life cycle; a reproductive stage called a trophozoite, and a dormant stage called a cyst. After an individual ingests a cyst, stomach acid triggers the hatching of two trophozoites (AWWA, 1985). The trophozoites multiply in the duodenum, jejunum and upper ileum by binary fission and, in a severe infection, attach themselves with a sucking disk to nearly every epithelial cell (Linn, 1985). The inability to absorb fats and other nutrients disrupts the normal intestinal activities, causing abdominal distention, diarrhea, flatulence, belching, nausea, vomiting, anorexia, fatigue, and cramps (AWWA, 1985). Periodically the trophozoites detach and travel through the bowel, forming cysts which are shed through the stools of the individual.

Recently, amendments to the Safe Drinking Water Act, public law 93-523, state that the EPA will promulgate criteria for (1) filtration of surface water supplies, and (2) disinfection for all water supplies in the U.S. The "surface water treatment rule" was proposed 3 November 1987, revised 6 May 1988, and finalized in the fall of 1988. It states that treatment must achieve at least 99.9% removal and/or inactivation of *Giardia* cysts and 99.99% removal and/or inactivation of enteric viruses. Water producers will be in violation if they do not conform by fall 1992. In order to comply, water treatment plants need a quick and efficient way to check their treated water.

Detection of *Giardia lamblia* cysts, be it for clinical diagnosis or water treatment purposes, exists in some commonly used techniques revolving around microscopic examination. They include bright-field microscopy such as staining, and indirect fluorescent antibody (IFA) methods. Bright-field microscopy is a tedious and time consuming procedure requiring individuals proficient in these areas. The IFA procedure results in an identification process specific to *Giardia* cysts that marks them with fluorescein isothiocyanate (FITC) dye via an antibody to *Giardia* cysts. The dye, which has its peak fluorescence near 535nm (green), simplifies the identification of the cysts (Nikon, 1985).

The objective of this project is to use the IFA method in conjunction with digital image processing techniques to create a cost effective instrumentation package that can automatically identify and count *Giardia lamblia* cysts and possibly help water producers meet the new water treatment regulations.

MATERIALS AND METHODS

Presently, our system consists of a Nikon Labophot Microscope in an epifluorescence configuration with a mercury light source and camera mount. A Computar series 3800 CCD (charged coupled device) black and white camera is placed on the camera mount to capture the magnified image. The relative light intensities of the image are converted to voltage signals and sent to a frame grabber which is housed in an AT&T 6300 computer. Here, the voltage signals are further converted to binary values between 0 to 63, with each value dictating a specific shade of gray; 0 represents the black end limit; 63 represents the white end limit. When these values are sent to a video monitor, they control the intensities of individual picture elements (pixels) to recreate a black and white "picture" of the image in view under the microscope.

IMAGE ENHANCEMENT

The frame grabber provides the added benefit of allowing video images to be altered for enhancing selected features. Image processing software has been written to allow only a selected band of intensities to be displayed, satisfactorily emphasizing or deemphasizing targeted objects. Linear contrast enhancement and bit-slicing are techniques that employ such tactics and are fundamental in the algorithms written for use in our project.

Briefly, linear contrast enhancement modifies a given band of intensities by calculating and using the proximity ratio of each intensity within the band relative to the entire dynamic range of intensity levels. This produces a prominent visual contrast in the video image. Bit-slicing takes a given band and converts only intensities in that band to full white saturation. Anything above or below this band is converted to full black saturation.

In all the cyst recognition methods developed, each requires the objects in the video to be in full white saturation (i.e., the intensity of every pixel in the object to be the binary equivalent of 63). This is the job of the bit-slicing technique. However, the proper range of intensities needs to be determined first so the cysts are emphasized while at the same time eliminating most, if not all, of the noncyst objects from

the data. Recognizing that the eye is not highly sensitive to gray scale variations, this was accomplished by investigating the raw video image of the cyst and acquiring the binary values of the pixels near its perimeter. A program was written especially for accessing the values of any pixel by moving a cursor controlled video cross-hair over the desired pixel. For the *Giardia lamblia* cyst in Fig. 1 which was taken at x1000 magnification, the near optimal band for bit-slicing is from six to 15. Fig. 2 is the result of bit-slicing within this band.

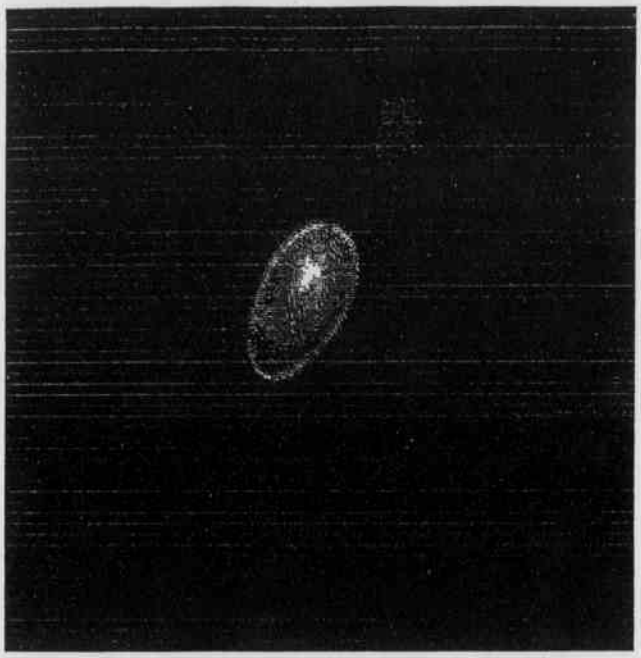

Figure 1. Image of fluorescing *G. lamblia* cyst at x1000 magnification.

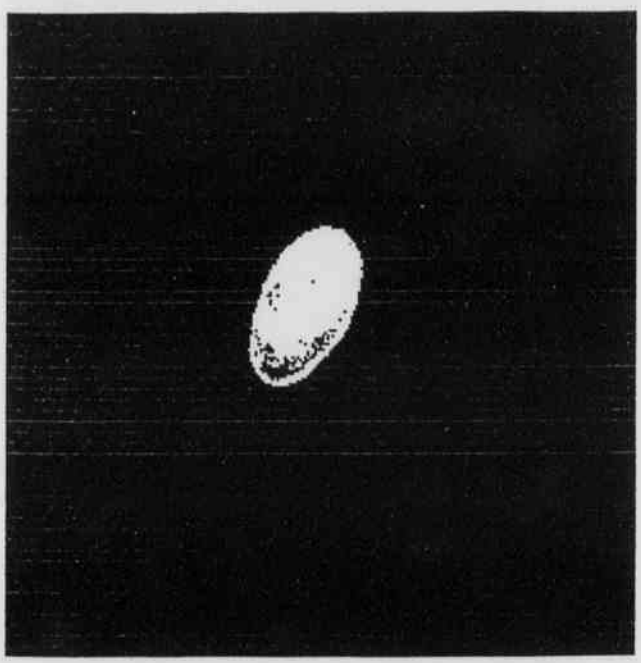

Figure 2. *G. lamblia* image modified by bit-slicing within an intensity band of 6 to 15.

The description of three methods that have been tried in the software development of an adequate *Giardia lamblia* cyst recognition algorithm follows. Area and perimeter calculations and cyst accumulation counts are automatically displayed on the computer monitor. The model cyst mentioned in these methods will eventually be created by taking the average areas and perimeters of a large sample of actual cysts. Because this project is still in the preliminary stages, the parameters of the model cyst were estimated from a small sample of cysts.

Method 1 assumes that the image contains no foreign objects after using the bit-slicing capabilities of the frame grabber. The ideal video image should reflect either a relatively black screen when no cysts are present or clusters of white pixels representing the effective areas of cysts (Fig. 2). By counting the total number of white pixels from the video image, dividing that by the number of pixels that make up the model cyst and allowing for slight variations in cyst size, the number of cysts in the image can be estimated. From experimental data, the model cyst at x1000 magnification has an effective area of approximately 2040 pixels. Although more data need to be taken, a difference of 40% from the model cyst pixel count is allowed. The area count for this cyst is 1725 pixels.

Method 2 introduces the comparison of perimeter pixel counts to achieve better cyst verification. This method was also designed around an ideal image. To save processing time, the computer program automatically locates the object on video and isolates it by placing a box of quarter-intensity pixels around it. Centering the box around the cyst is accomplished by finding the first and last rows the cyst occupies and calculating the row halfway between these two outer rows. This center row is scanned to find the first and last pixels, whereby the pixel midway between the two outer pixels is calculated and the box is centered around this pixel. The interior of the box is scanned first by columns, then by rows, to identify the first and last pixels it encounters to mark with half-intensity pixels indicating the perimeter of the cyst. Finally, all pixels within the box are inspected (Fig. 3). The number of half-

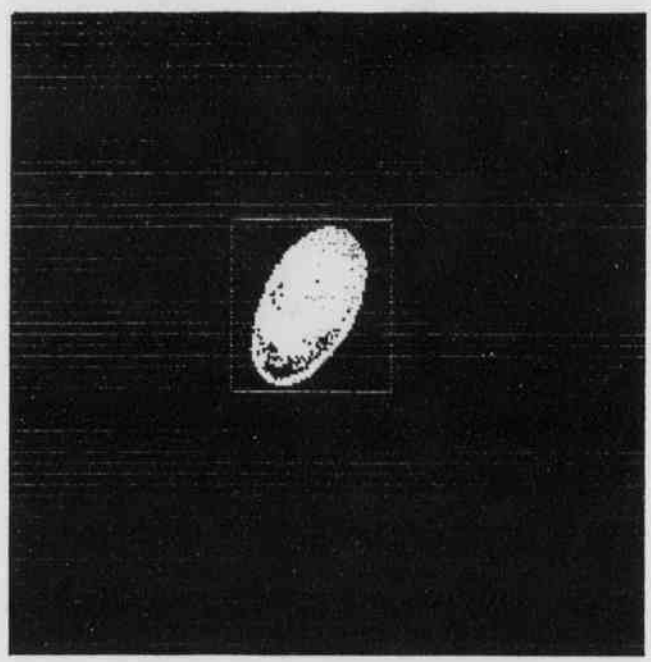

Figure 3. *G. lamblia* image processed using Method 2.

intensity pixels is the perimeter count and the combined number of half-intensity and full-intensity pixels is the area count. By dividing these numbers by area and perimeter counts of the model cyst — 2040 pixels and 146 pixels, respectively — it is concluded whether or not the object is a cyst. Again, variation in cyst size was considered. A 40% difference from the area and a 20% difference from the perimeter of

the model cyst was allowed. For the cyst in Fig. 3 the area count is 1725 pixels and the perimeter count is 144 pixels.

Method 3 considers the more likely image where background objects will be present regardless of the extensive use of processing techniques to emphasize the cysts (Kitchin *et al.*, 1983).

Before this method is implemented, the image is first processed using an automated ends-in search contrast enhancement algorithm which was recently integrated into this method. It looks at the histogram of pixel intensities of the video image, analyzes it, and performs linear contrast enhancement in a range of intensities relative to a predetermined percentage of pixels to be saturated either black or white as calculated from the cumulative distribution function. The cumulative distribution function represents the percentage of pixels with intensities at or below a given intensity (Green, 1989). After some trial and error, it was determined that the lower intensity limit be 3.17% below 100% (i.e., the intensity where 96.83% of the pixels have intensities below this intensity), and the upper intensity limit be at 100%. This corresponds to an intensity band from five to 15 over which the linear contrast enhancement is performed. Once this is completed, the image is bit-sliced over the entire range of pixel intensities leaving the remaining objects as clusters of white pixels (Fig. 4).

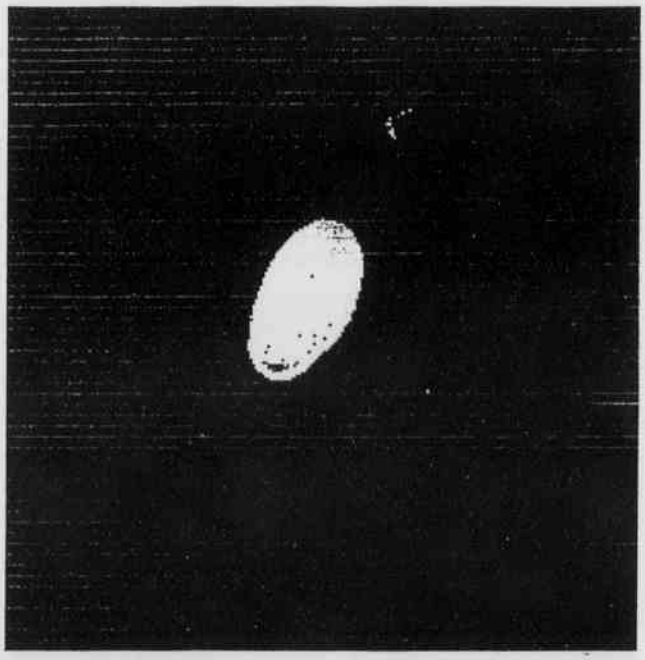

Figure 4. Results of using linear contrast enhancement and bit-slicing in Method 3.

The next step is to create an edge matrix of half-intensity pixels in a second 64K memory area which represents possible perimeters of objects in the current image. Each pixel is organized to be the upper left pixel (hereafter called the primary pixel) of a group of four pixels. Organizing them as such requires the groups to overlap each other, assuring a continuous transition into the edge matrix. Each group of four pixels is compared to four specific pixel patterns representing cases where the primary pixel cannot be regarded as the exterior of an object. If no match is made, the primary pixel is indicated as an edge with a half-intensity pixel in the edge matrix. This continues until the last group of four pixels in the image is analyzed. The edge matrix is then swapped with the image on video (Fig. 5). Each pixel in the current video is inspected until it reaches a half-intensity pixel assumed to be the perimeter of an object from the image. From this pixel a specific vector search pattern which moves in a counter-clockwise direction is used to locate the next half-intensity pixel. Eight different vector directions are allowed in a search (Fig. 6). The decision on which vector direction will

Figure 5. Corresponding edge matrix to image in Figure 4.

begin the search depends on the last vector movement that found the current perimeter pixel (Figs. 6 & 7). Upon identifying the next half-intensity pixel, it is changed into a full-intensity pixel. This continues until the search returns to the originating perimeter pixel of the object. The next object is located and the vector search is repeated (Fig. 8).

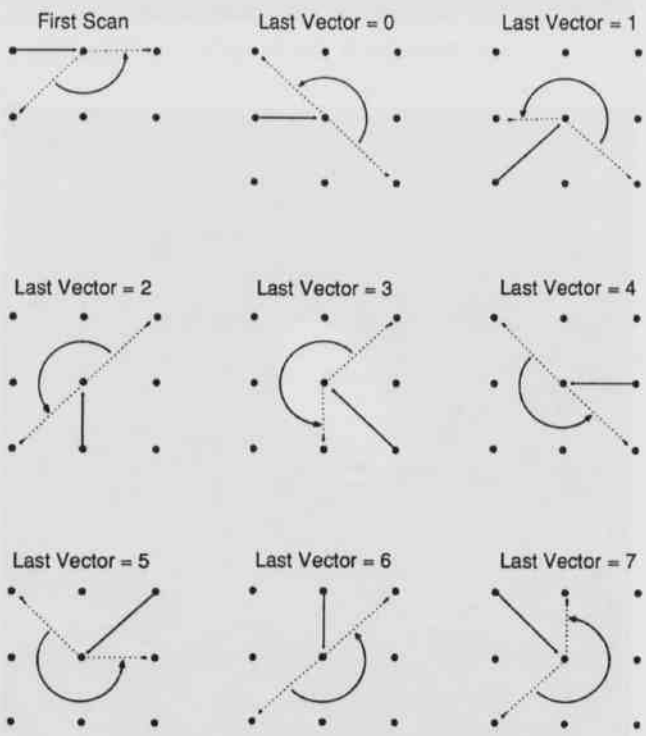

Figure 6. Vector search patterns used in determining the outer boundaries of objects in the edge matrix.

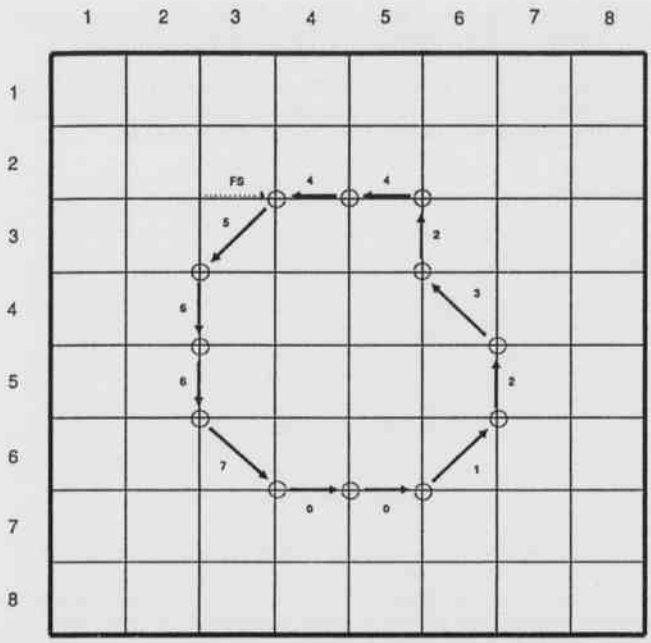

Figure 7. An example of the direction of movement during a vector search. The numbers adjacent to each vector represents the last vector number. FS = First Scan.

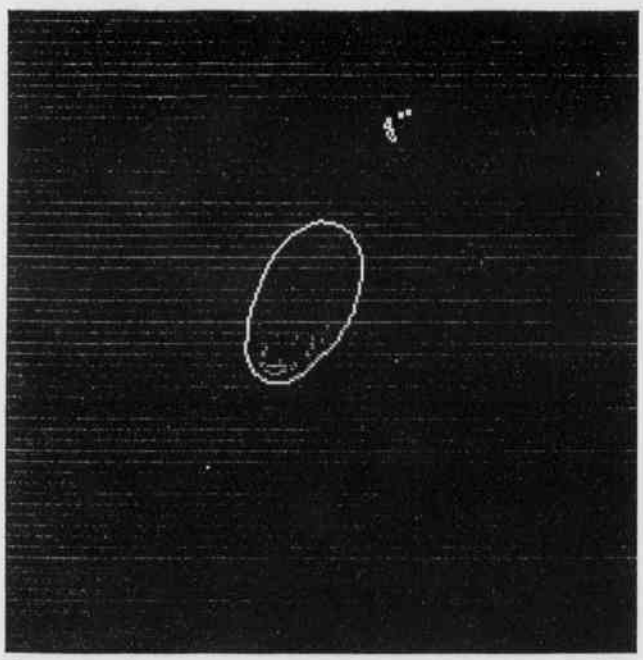

Figure 8. Result of the completed vector search used in Method 3.

Each of the directional vectors also serves to calculate the area and perimeter of the object. As each vector is determined, the designated vector numbers are used in area and perimeter formulas (Fig. 9). Notice that the formulas consider a pixel to be a unit square and consequently factors in a square root of two when taking the diagonal halves of pixels. From experimentation, at x400 magnification, the model cyst area is 316.0 pixels and the model cyst perimeter is 73.0 pixels. At x1000 magnification, the model cyst area is 1974.5 pixels and the model cyst perimeter is 174.7 pixels. Once the area and perimeter have been completely calculated, they are checked to see if they comply with the parameters of the model cyst. If so, the object is counted as a cyst. For the cyst in Fig. 4 the area count is 935.5 pixels and the perimeter count is 175.9 pixels.

$$\text{Perimeter} = \sum \begin{cases} P + 1 & \text{if edge vector is even} \\ P + \sqrt{2} & \text{if edge vector is odd} \end{cases}$$

$$\text{Area} = \sum \begin{cases} Y & \text{if edge vector} = 0 \\ Y - 1/2 & \text{if edge vector} = 1 \\ 0 & \text{if edge vector} = 2 \\ -(Y - 1/2) & \text{if edge vector} = 3 \\ -Y & \text{if edge vector} = 4 \\ -(Y + 1/2) & \text{if edge vector} = 5 \\ 0 & \text{if edge vector} = 6 \\ Y + 1/2 & \text{if edge vector} = 7 \end{cases}$$

Figure 9. Formulas used in calculating the perimeter and area during the vector search.

RESULTS AND DISCUSSION

Methods 1 and 2 can only be successful in the ideal situation, when all background objects have been eliminated using image processing techniques and only cysts are expected to remain. Additionally, method 1 can accommodate multiple cysts per image. However, method 2, unless further improved, can only deal with one cyst per screen as the algorithm is incapable of successive searches in the same image.

Method 3 is the most flexible as it can search the entire screen and, by process of elimination, determine what is a cyst and what represents foreign objects. Its perimeter and area calculations are more accurate because of the consideration of rounded objects to which it adjusts by using the diagonal halves of pixels. Methods 1 and 2 do not make a similar adjustment.

It is anticipated that further developments may lead to additional methods which require identifying the morphology of the cysts for proper recognition, and this may depend on the environment in which the cysts are extracted; e.g., surface water, giardiasis patients. However, in certain situations, one of the above methods might suffice. Future testing is needed to confirm this.

During the development of the project, certain unexpected factors regarding the environment in which the *Giardia* cysts were extracted became a stumbling block in the attempts to make the image processing based solely on fluorescence intensity. Some of the organic materials that are companion to the cysts have natural fluorescence, but of a different color. Therefore, plans are to include color differentiation using selected filters as part of the system.

Another long-term goal is to fully automate the system by employing a computer to control stage and focus movement of the epi-fluorescence microscope. While processing prepared slides of *Giardia* cysts, it would be ideal to store the coordinates of the locations of identified cysts to memory so that one can quickly send the stage to the proper position and access the cysts for normal microscopic viewing or, if equipped, for viewing under Nomarski differential interference contrast (DIC) microscopy.

LITERATURE CITED

AMERICAN WATER WORKS ASSOCIATION (AWWA). 1985. Waterborne *Giardia:* it's enough to make you sick. J. AWWA. 77:14, 19, 22, 26, 84.

GREEN, W.B. 1989. Digital image processing. Van Nostrand Reinhold, New York.

KITCHIN, P.W. and A. PUGH. 1983. Processing of binary images. Pp. 21-42, in A. Pugh (ed.) Robot Vision. IFS (Publications) Ltd., U.K.

LIN, S.D. 1985. *Giardia lamblia* and water supply. J. AWWA. 77:40-47.

NIKON. 1985. Spectrum absorption and emittance of leading fluorochromes. Nikon fluorescence microscopes (brochure).

POLIS, M.A., C.U. TUAZON, D.W. ALLING, and E. TALMANIS. 1986. Transmission of *Giardia lamblia* from a day care center to the community. Am. J. Pub. Health. 76:1142-1144.